

See discussions, stats, and author profiles for this publication at: <https://www.researchgate.net/publication/51543331>

Comprehensive Structural Analysis of Mutant Nucleosomes Containing Lysine to Glutamine (KQ) Substitutions in the H3 and H4 Histone-Fold Domains

ARTICLE *in* BIOCHEMISTRY · AUGUST 2011

Impact Factor: 3.02 · DOI: 10.1021/bi201021h · Source: PubMed

CITATIONS

17

READS

48

6 AUTHORS, INCLUDING:



Hiroaki Tachiwana

Waseda University

39 PUBLICATIONS 591 CITATIONS

[SEE PROFILE](#)



Wataru Kagawa

Meisei University

48 PUBLICATIONS 1,341 CITATIONS

[SEE PROFILE](#)

Comprehensive Structural Analysis of Mutant Nucleosomes Containing Lysine to Glutamine (KQ) Substitutions in the H3 and H4 Histone-Fold Domains

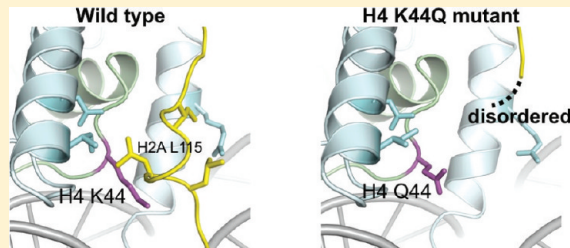
Wakana Iwasaki,^{†,‡,§} Hiroaki Tachiwana,^{†,§} Koichiro Kawaguchi,[†] Takehiko Shibata,[‡] Wataru Kagawa,[†] and Hitoshi Kurumizaka^{*,†}

[†]Laboratory of Structural Biology, Graduate School of Advanced Science and Engineering, Waseda University, Shinjuku-ku, Tokyo 162-8480, Japan

[‡]RIKEN Advanced Science Institute, 2-1 Hirosawa, Wako-shi, Saitama 351-0198, Japan

Supporting Information

ABSTRACT: Post-translational modifications (PTMs) of histones play important roles in regulating the structure and function of chromatin in eukaryotes. Although histone PTMs were considered to mainly occur at the N-terminal tails of histones, recent studies have revealed that PTMs also exist in the histone-fold domains, which are commonly shared among the core histones H2A, H2B, H3, and H4. The lysine residue is a major target for histone PTM, and the lysine to glutamine (KQ) substitution is known to mimic the acetylated states of specific histone lysine residues *in vivo*. Human histones H3 and H4 contain 11 lysine residues in their histone-fold domains (five for H3 and six for H4), and eight of these lysine residues are known to be targets for acetylation. In the present study, we prepared 11 mutant nucleosomes, in which each of the lysine residues of the H3 and H4 histone-fold domains was replaced by glutamine: H3 K56Q, H3 K64Q, H3 K79Q, H3 K115Q, H3 K122Q, H4 K31Q, H4 K44Q, H4 K59Q, H4 K77Q, H4 K79Q, and H4 K91Q. The crystal structures of these mutant nucleosomes were determined at 2.4–3.5 Å resolutions. Some of these amino acid substitutions altered the local protein–DNA interactions and the interactions between amino acid residues within the nucleosome. Interestingly, the C-terminal region of H2A was significantly disordered in the nucleosome containing H4 K44Q. These results provide an important structural basis for understanding how histone modifications and mutations affect chromatin structure and function.



In eukaryotic chromosomes, genomic DNA is organized into chromatin. The elemental repeating unit of chromatin is the nucleosome core particle (NCP), which consists of 146 base pairs of DNA wrapped in 1.65 left-handed superhelical turns around the histone octamer.¹ The histone octamer comprises two each of the core histones, H2A, H2B, H3 and H4, which form two H2A/H2B dimers and an H3/H4 tetramer, respectively, in the NCP. These core histones share common structural motifs, in which the central histone-fold domain is bordered by flexible N- and C-terminal tails.^{2,3}

Histones are subjected to a plethora of post-translational modifications (PTMs), including acetylation of lysines, methylation of lysines and arginines, phosphorylation of serines and threonines, ADP-ribosylation of glutamic acids, ubiquitylation and SUMOylation of lysines, and biotinylation of lysines. Until recently, the unstructured N-terminal histone tails have been considered to be the primary substrate for diverse PTMs. On the basis of these findings, the histone code hypothesis was proposed, which states that the presence of defined patterns of modifications on the flexible histone tails alters the accessibility of effector proteins to the nucleosomal DNA.^{4,5} This system is predicted to regulate gene expression epigenetically, in combination with histone variant exchange.^{6,7}

Advanced mass spectrometric studies have identified a number of novel modifications in the histone-fold domains of core histones.^{8–11} Consgrove et al. reported that many of these modification sites are located on the histone–DNA contact surface and proposed a “regulated nucleosome mobility” model, in which the equilibrium between low mobility and high mobility nucleosomes is regulated by changes in the histone–DNA binding affinity through the histone modifications.¹² In this model, the ATP-dependent nucleosome-remodeling factors and the histone acetylations cooperatively weaken histone–DNA contacts and increase nucleosome mobility. On the other hand, the removal of the acetyl group from acetylated histones by deacetylases restores histone–DNA contacts and decreases nucleosome mobility.¹² In addition to the modifications on the histone–DNA contact surface, Mersfelder and Parthun reviewed those at other locations on the histone-fold domains and discussed their roles in the regulation of chromatin structure.¹³

Lysine acetylation, a major histone PTM, neutralizes the positive charge of the ε-amino group of the side chain by

Received: July 4, 2011

Revised: July 30, 2011

Published: August 3, 2011

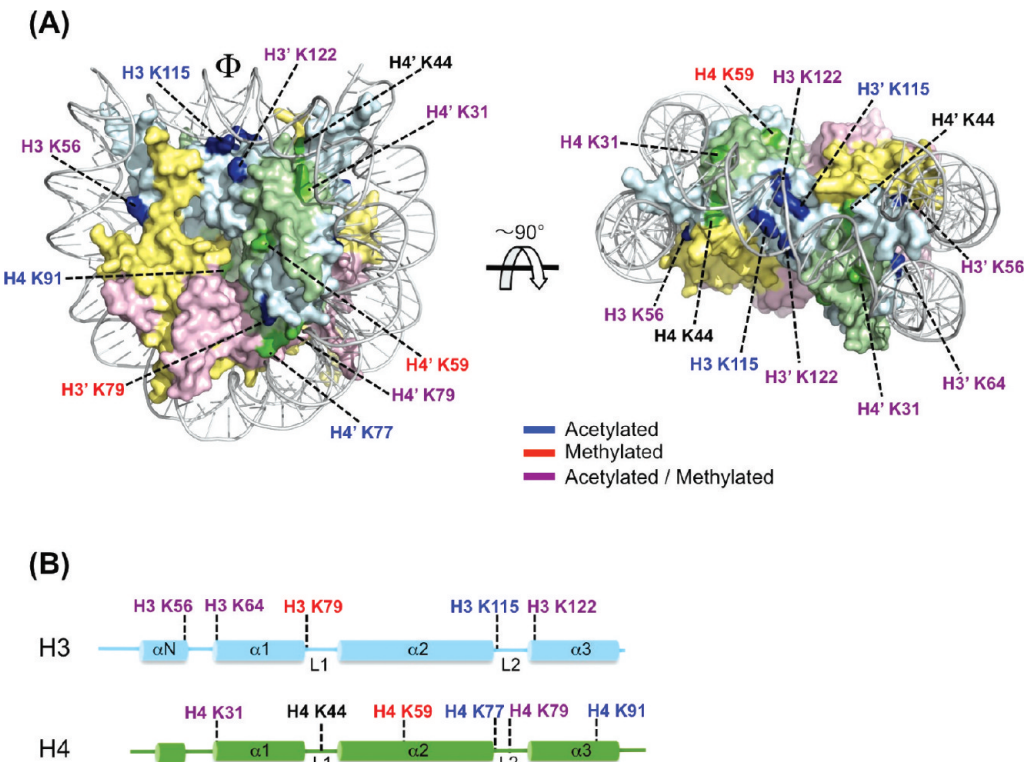


Figure 1. (A) Surface representation of the human NCP (PDB code 3AFA). Histone H3 is colored cyan, H4 is pale green, H2A is yellow, H2B is pink, and DNA is gray. The H3 and H4 lysine residues mutated to glutamine are shown in blue and green, respectively. The lysine residues identified as targets for acetylation, methylation, and acetylation/methylation are labeled in blue, red, and purple, respectively. The location of the dyad axis is indicated by Φ . (B) Secondary structures of histones H3, and H4. The lysine residues substituted with glutamine are labeled as in panel A.

adding an acetyl group. Neumann et al. established a system for the site-specific incorporation of *N*-acetyllysine in recombinant proteins, using an *N*-acetyllysyl-tRNA synthetase/tRNA pair.^{14,15} The site-specific incorporation of acetyllysine at position 56 of histone H3 was also established by a chemical ligation strategy.¹⁶ On the other hand, site-directed mutagenesis to replace lysine with glutamine has been used as a concise method to mimic lysine acetylation. *In vivo*, the lysine replacement by glutamine or asparagine partially mimics the functions of acetylated histones.^{17,18} Consistently, glutamine substitutions in the tail domains of histones were demonstrated to have effects similar to acetylation on higher-order chromatin structure.¹⁹ Therefore, the histone KQ mutants, in which the lysines (K) are replaced by glutamines (Q), are important tools for understanding the functional significance of histone acetylation. However, the nucleosome structures containing the KQ mutations of core histones have not been reported, except for the histone H3 K56Q mutant.²⁰

To obtain comprehensive structural information for the nucleosomes containing histone KQ mutants, in the present study we prepared 11 mutant NCPs, in which each of the lysines in the histone-fold domains of human histones H3 and H4 was replaced by glutamine (Figure 1). We then determined the crystal structures of these mutant NCPs and discussed their structural characteristics.

EXPERIMENTAL PROCEDURES

Preparation and Crystallization of NCPs. Previously reported protocols were used to express, purify, and reconstitute the mutant NCPs.²¹ Crystals for all of the mutants were obtained by the hanging drop vapor diffusion method,

using 20 mM potassium cacodylate (pH 6.0), 40–50 mM KCl, and 60–120 mM MnCl₂ as the crystallization solution. Drops composed of 1 μ L of nucleosome solution and 1 μ L of crystallization solution were equilibrated against 500 μ L of reservoir solution, containing 20 mM cacodylate (pH 6.0), 35–40 mM KCl, and 40–70 mM MnCl₂, at 20 °C.

Crystallographic Data Collection and Structure Determination. The diffraction data were collected at BL41XU of SPring-8 at a wavelength of 1.0 Å. Crystals were soaked in cryoprotectant solutions containing 20 mM potassium cacodylate (pH 6.0), 40 mM KCl, 55 mM MnCl₂, 28% 2-methyl-2,4-pentandiol, and 2% trehalose and were flash-cooled in a stream of nitrogen gas at 100 K. The data were indexed, integrated, and scaled with HKL2000²² and were further processed using CCP4 suite programs.²³ All structures were solved by the molecular replacement method with the program MOLREP,²⁴ using the human NCP structure (Protein Data Bank code 2CV5) as the search model. All models were checked using sigma-A-weighted omit maps during the early stages of the modeling. The models were rebuilt with COOT²⁵ and refined with CNS.²⁶ The statistics for data collection and refinement are shown in Table 1. All molecular graphics images were generated using PyMOL.²⁷

RESULTS AND DISCUSSION

Human histone H3.1 mutants, containing the single amino acid substitutions H3 K56Q, H3 K64Q, H3 K79Q, H3 K115Q, and H3 K122Q, were purified as recombinant proteins by the method described previously.^{21,28} Similarly, human histone H4 mutants, containing the single amino acid substitutions H4 K31Q, H4 K44Q, H4 K59Q, H4 K77Q, H4 K79Q, and H4

Table 1. Data Collection and Refinement Statistics

	crystal data	H31 ^a	H3 K56Q	H3 K64Q	H3 K115Q	H3 K122Q	H4 K31Q	H4 K77Q	H4 K91Q	H3 K79Q	H4 K59Q	H4 K44Q
<i>data collection statistics</i>												
unit-cell parameters ^b												
<i>a</i> (Å)	105.8	106.0	106.1	106.5	106.1	106.4	106.6	106.4	106.6	106.5	106.6	106.0
<i>b</i> (Å)	109.5	109.5	109.3	109.8	109.7	109.5	109.6	108.8	109.7	109.8	109.4	109.4
<i>c</i> (Å)	180.9	181.6	175.8	182.4	181.8	176.0	182.2	174.5	182.1	182.2	182.6	180.9
resolution range (Å)	50.0–2.50	50.0–2.90	50.0–3.00	50.2–2.40	50.0–3.50	50.0–2.70	50.0–2.70	50.2–2.90	50.0–3.01	50.0–2.70	50.0–3.20	50.0–2.90
no. of reflections	518 622	233 760	294 801	604 608	184 616	404 743	434 476	309 182	307 779	443 648	224 684	348 558
no. of unique reflections	73 546	41 028	41 758	84 116	27 471	56 801	59 340	44 914	42 940	59 548	35 150	47 901
completeness (%) ^c	99.8 (99.5)	86.2 (82.5)	99.8 (99.9)	99.7 (99.5)	99.7 (99.8)	99.6 (99.5)	99.9 (100)	99.3 (97.1)	99.9 (100)	97.8 (90.4)	99.9 (100)	99.9 (100)
<i>R</i> _{sym} (%) ^{c,d}	7.7 (60.1)	9.5 (71.2)	8.9 (40.7)	8.5 (76.8)	10.2 (27.9)	8.1 (62.8)	7.2 (48.1)	9.2 (87.0)	10.4 (62.4)	8.4 (55.5)	5.6 (25.9)	9.8 (60.6)
<i>I</i> / σ (<i>I</i>) ^e	13.4 (4.2)	12.1 (2.5)	11.5 (5.7)	10.7 (2.9)	8.3 (6.5)	11.4 (3.3)	12.6 (5.3)	9.7 (2.6)	11.1 (4.5)	10.3 (4.4)	22.1 (11.0)	11.1 (4.5)
<i>refinement statistics</i>												
<i>R</i> _{work} (%) ^e / <i>R</i> _{free} (%)	25.2/27.9	21.8/27.3	24.4/30.2	22.6/26.8	19.0/26.6	23.0/28.9	20.8/25.9	24.1/29.6	19.7/25.4	21.3/26.3	20.0/25.7	22.0/26.8
no. of protein residues	758	755	756	757	755	759	760	755	758	756	759	742
no. of base pairs of DNA	146	145	146	145	145	145	145	145	145	145	145	145
no. of ions	12	15	14	13	15	17	15	10	15	16	15	16
no. of water molecules	183	0	0	103	0	73	164	0	0	198	0	0
rmsd from ideal bond length (Å)	0.006	0.006	0.006	0.008	0.007	0.007	0.007	0.007	0.006	0.007	0.007	0.008
bond angles (deg)	1.11	1.17	1.11	1.23	1.21	1.16	1.24	1.21	1.13	1.17	1.20	1.32
<i>av B-factors (Å²)</i>												
protein	37.0	48.8	56.3	43.3	38.3	64.0	49.9	73.3	42.0	41.3	46.0	34.4
DNA	92.4	104.1	124.9	98.5	96.1	124.5	101.1	135.0	95.2	99.6	104.9	89.3
ion	67.3	85.3	96.3	75.3	78.7	120.5	86.7	106.0	76.8	83.6	83.4	71.9
solvent	35.4			37.8		49.8	43.6			38.5		
PDB code	3AFA	3AYW	3AZE	3AZH	3AZI	3AZL	3AZM	3AZN	3AZF	3AZK	3AZJ	
<i>rmsd with wild type</i>												
<i>C</i> _α (histones) (Å)	0.29	0.39	0.32	0.39	0.40	0.23	0.41	0.28	0.22	0.33	0.28	
P (DNA)(Å)	0.65	0.98	0.56	0.68	0.93	0.49	0.88	0.47	0.63	0.52	0.54	

^aData of the previously reported wild type prepared by the similar method to that of mutants are shown for comparison.²¹ ^bAll the crystals belong to the same space group *P*2₁2₁2₁ as wild type. ^cValues in parentheses are for the highest-resolution shell. ^d*R*_{sym} = $\sum_{hkl} \sum_i |I_{hkl,i} - \langle I_{hkl} \rangle| / \sum_{hkl} \sum_i |I_{hkl,i}|$. ^e*R*_{work} = $\sum_{hkl} |F_{0,i}| - |F_{c,i}| / \sum_{hkl} |F_{0,i}|$. *R*_{free} is calculated with 5% of the total reflections held aside throughout the refinement.

K91Q, were prepared. Each of these H3 and H4 mutants was incorporated into NCPs by the salt-dialysis method,^{21,29} and the NCPs were purified by native polyacrylamide gel electrophoresis.³⁰ The crystals of all of the mutant NCPs belonged to the space group $P2_12_12_1$, and the structures were determined at resolutions ranging from 2.4 to 3.5 Å, as summarized in Table 1. In these mutant NCP structures, the electron densities for the glutamines, which replaced the lysines, were sufficiently visible for model building (Figure S1).

For structural comparison, the crystal structure of human NCP at 2.5 Å resolution (PDB code 3AFA),^{21,29} obtained by the same sample preparation method as that for the mutant NCPs, was used as the wild-type NCP structure. The rmsd's between the wild-type and mutant NCP structures were calculated by superimpositions on all phosphorus atoms of the DNA and all $C\alpha$ atoms of the histones. To reduce the effect of the crystal packing environment, the rmsd values were averaged between the two copies of each histone pair. The high-resolution crystal structure of *Xenopus laevis* NCP determined at 1.9 Å (PDB code 1KX5),³¹ which contains over 3000 water molecules, was also used when information about solvent-mediated interactions was required for the structural comparison. Since the DNA-binding path of the *X. laevis* NCP is locally altered, as compared to that of the human NCPs,^{21,32} the DNA regions altered between the human and *X. laevis* NCPs were not included in our comparison.

We first analyzed the eight mutant nucleosomes containing H3 K56Q, H3 K64Q, H3 K115Q, H3 K122Q, H4 K31Q, H4 K77Q, H4 K79Q, and H4 K91Q. These lysine residues are reportedly acetylated. Three more nucleosome structures, representing the H3 K79Q, H4 K59Q, and H4 K44Q mutants, whose acetylations have not been reported, are also described.

Structure of the H3 K56Q Mutant NCP. The acetylation of the H3 K56 residue has been intensely investigated due to its critical role in regulating transcription, replication, chromatin assembly, and DNA repair.^{33–37} This acetylation is a mark of newly synthesized histone H3 during S phase, and it is removed during the G2 and M phases.^{33,34} However, the H3 K56 acetylation persists in the presence of DNA damage, suggesting that it creates a favorable chromatin environment for DNA repair.³³ The H3 K56 residue is located on the N-terminal helix (α N) (Figure 1). Watanabe et al. determined the crystal structure of the *X. laevis* NCP containing the H3 K56Q mutant at 3.8 Å resolution and showed that the mutation has no detectable effects on the structure of the nucleosome.²⁰ In this study, we determined the crystal structure of the human NCP containing the H3 K56Q mutant at 2.9 Å resolution. The electron density for the side chain of glutamine at position 56 in the H3 K56Q *Xenopus* NCP was reportedly invisible, probably due to its low resolution.²⁰ In contrast, in the human NCP, the electron density of the H3 Q56 side chain is clearly observed, allowing us to determine the side-chain orientation (Figure S1). The water-mediated contacts between the H3 K56 residue and DNA in the wild-type NCP (Figure 2A) are lost in the H3 K56Q mutant NCP (Figure 2B) because the orientation of the H3 Q56 side chain differs from that of the wild-type H3 K56 side chain.

Watanabe et al. demonstrated that the H3 K56Q mutation destabilizes cooperative, interarray interactions, when the arrays contain nucleosome-free regions, although it does not affect short-range nucleosome–nucleosome interactions within a single nucleosomal array.²⁰ Single-molecule FRET experiments

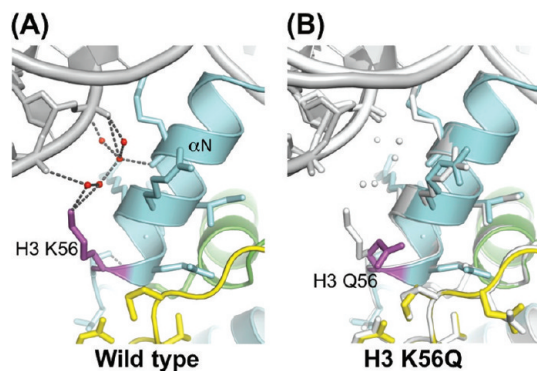


Figure 2. Structures of the H3 K56Q mutant NCP. (A) Close-up view of the structure around the H3 K56 residue of the wild-type NCP. (B) Close-up view of the structure of the H3 K56Q mutant NCP. Histones H3 and H4 are colored cyan and green, respectively. Hydrogen bonds and salt bridges are denoted by dashed lines. In panel B, the wild-type structure is superimposed and shown in white for comparison. The H3 K56 (A) and H3 Q56 (B) residues are shown in magenta. Water molecules mediating hydrogen bonds are depicted as red spheres.

revealed that the H3 K56 acetylation increases the “breathing” (partial unwrapping) of DNA.¹⁵ In the orthorhombic crystals of the wild-type NCP and all mutant NCPs, the DNA ends of the adjacent NCPs are packed end-to-end, forming a pseudocontinuous double helix (data not shown).¹ These crystal packing contacts may prevent the transient unwrapping of the DNA ends in the crystal structure, as also suggested in the previous report.²⁰ Partial unwrapping of the DNA ends was observed in the crystal structure of the centromeric nucleosome containing CENP-A.³⁸ The CENP-A nucleosome crystal belonged to the space group $P2_1$, in contrast to the typical orthorhombic $P2_12_12_1$ crystals of the canonical H3 nucleosomes. The occurrence of the transient unwrapping of the DNA ends in crystals may depend on the space group.

Structure of the H3 K64Q Mutant NCP. The H3 K64 residue is known to be acetylated, but its biological significance has not been determined.^{39,40} This residue is also reportedly trimethylated, enriched at pericentric heterochromatin, and dynamically regulated during developmental reprogramming in mammals.⁴¹ The H3 K64 residue is located on the N-terminal side of the H3 α 1 helix (Figure 1). In the structure of the wild-type NCP, the main-chain amide nitrogen of the H3 K64 residue hydrogen bonds with the DNA phosphates, and the H3 K64 side-chain Ne forms a hydrogen bond network mediated by water molecules that would contribute toward stabilizing the arrangement of the H3 α 1 and α 2 helices (Figure 3A). The former hydrogen bonds with DNA are present in the structure of the H3 K64Q mutant NCP (Figure 3B). Although the 3.0 Å resolution data for the H3 K64Q NCP are insufficient to confirm the absence of hydrated water molecules, the latter hydrogen bond network may be disrupted in the mutant because the orientation of the glutamine side chain of the H3 Q64 residue is quite different, as compared to that of the wild-type H3 K64 residue (Figure 3). The structural data suggest that the side chain of the acetylated H3 K64 residue should be oriented in a similar manner to that of the H3 Q64 side chain to avoid steric conflict between the acetyl moiety and the H3 Q64 side chain (Figure 3). Thus, the acetylation of the H3 K64 residue is presumed to disrupt the hydrogen bond network between the H3 α 1 and α 2 helices, as revealed in the H3 K64Q mutant NCP structure.

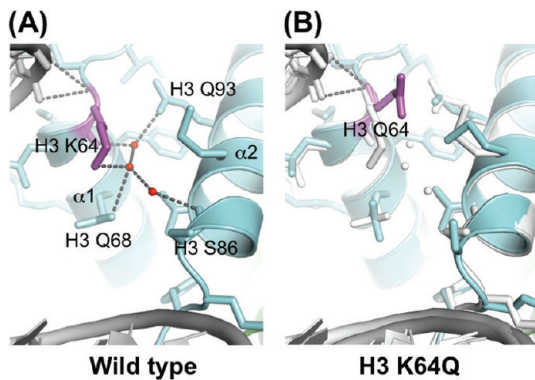


Figure 3. Structures of the H3 K64Q mutant NCP. (A) Close-up view of the structure around the H3 K64 residue of the wild-type NCP. (B) Close-up view of the structure of the H3 K64Q mutant NCP. Histone H3 is colored cyan. Hydrogen bonds and salt bridges are denoted by dashed lines. In panel B, the wild-type structure is superimposed and shown in white for comparison. The H3 K64 (A) and H3 Q64 (B) residues are shown in magenta. Water molecules mediating hydrogen bonds are depicted as red spheres.

Structures of the H3 K115Q and H3 K122Q Mutant NCPs. The H3 K115 and H3 K122 residues are located near the nucleosome dyad and have been identified as the targets for acetylation.¹⁰ Since the H3 K115 and H3 K122 residues both reside near the pseudo-2-fold axis, two symmetric pairs of these residues are clustered together (Figure 1A). The peptide mass fingerprinting analysis revealed that the H3 K115 and H3 K122 residues could be simultaneously acetylated.¹⁰ The flanking H3 R116 and H3 T118 residues have been identified as the sites for a SWI/SNF-independent (Sin) mutation that alleviates the transcriptional defects associated with the inactivation of the SWI/SNF chromatin remodeling complex.⁴² The Sin mutation destabilizes histone–DNA interactions.^{43–45} Although it is not known whether a mutation at the H3 K115 or H3 K122 residue leads to a Sin phenotype, a competitive reconstitution analysis revealed that the acetylation of the H3 K115 or H3 K122 residue reduces the free energy of the histone octamer binding to DNA.⁴⁶ Unlike the acetylation of the H3 K115 or K122 residue, the free energy is not altered by the H3 K115Q or H3 K122Q mutation, suggesting that these mutations may not fully mimic the effect of acetylation.⁴⁶ However, the H3 K115Q and H3 K122Q mutations reportedly exhibited distinct phenotypes in *Saccharomyces cerevisiae*: the H3 K115Q and H3 K122Q mutations each reduced transcriptional silencing at telomeres and rDNA.⁴⁷

The H3 K115 and H3 K122 residues are both involved in the same salt bridge network with the oxygen atoms of the DNA phosphate backbone, in the structure of the *Xenopus* NCP (Figure 4A,C).³¹ The structures of the H3 K115Q and H3 K122Q mutant NCPs were determined at 2.4 and 3.5 Å resolutions, respectively, and neither waters nor contacts around the mutation sites were observed (Figure 4B, D). A pronounced *B*-factor increase was not found for either the DNA or histone atoms. The overall structure of the H3 K115Q mutant NCP is almost identical to that of the wild-type NCP (data not shown). On the other hand, the residues with relatively high rmsd values were sparsely distributed on the surface of the H3 K122Q mutant NCP (Figure 4E, labeled residues). Consistently, the H3 K122 acetylation modestly increased the rate of thermal repositioning of the NCP along the DNA, whereas the H3 K115 acetylation did not change the

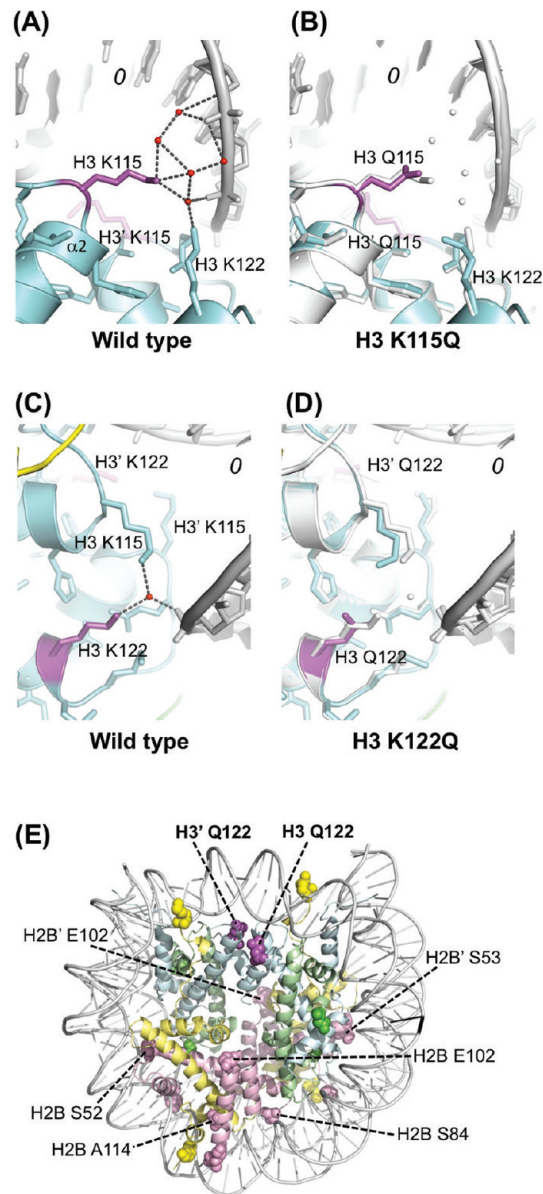


Figure 4. Structures of the H3 K115Q and H3 K122Q mutant NCPs. (A, B) Close-up views of the structures around the H3 K115 residue of the wild-type NCP (A) and the H3 K115Q mutant NCP (B). The H3 K115 (A) and H3 Q115 (B) residues are shown in magenta. (C, D) Close-up views of the structures around the H3 K122 residue of the wild-type NCP (C) and the H3 K122Q mutant NCP (D). The H3 K122 (C) and H3 Q122 (D) residues are shown in magenta. Histone H3 is colored cyan. Hydrogen bonds and salt bridges are denoted by dashed lines. In panels B and D, the wild-type structure is superimposed and shown in white for comparison. (E) Overall structure of the H3 K122Q mutant NCP. Histone subunits are colored as follows: H3 is cyan, H4 is green, H2A is yellow, and H2B is pink. The nucleotides with rmsd's ≥ 1.5 Å, as compared with the structure of the wild-type NCP, are shown in black. Similarly, the histone residues with rmsd's ≥ 0.6 Å are shown in space-filling representation. Flexible tail regions with rmsd's ≥ 0.6 Å are not labeled, for clarity. The H3 Q122 residues are depicted as magenta space-filling models.

rate.⁴⁶ Therefore, the modification or mutation of the H3 K122 residue may enhance the nucleosome mobility.

Structure of the H4 K31Q Mutant NCP. The H4 K31 residue has been identified as a site for acetylation and

methylation.⁴⁸ This site was hyperacetylated in a mouse model of lupus disease by an *in vivo* treatment with a histone deacetylase inhibitor.⁴⁸ The H4 K31 residue is located at the N-terminus of the H4 $\alpha 1$ helix (Figure 1B), and its side chain is extended in the major groove of the DNA (Figure 5A). The

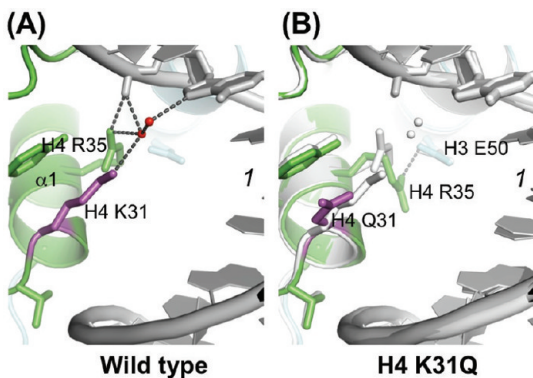


Figure 5. Structures of the H4 K31Q mutant NCP. (A) Close-up view of the structure around the H4 K31 residue of the wild-type NCP. (B) Close-up view of the structure of the H4 K31Q mutant NCP. Histone H4 is colored green. Hydrogen bonds and salt bridges are denoted by dashed lines. In panel B, the wild-type structure is superimposed and shown in white for comparison. The H4 K31 (A) and H4 Q31 (B) residues are shown in magenta. Water molecules mediating hydrogen bonds are depicted as red spheres.

side-chain $\text{N}\varepsilon$ forms a water-mediated salt bridge with the DNA phosphate backbone and a hydrogen bond with the guanine N7 amino group. These bonds seem to be disrupted in the H4 K31Q mutant NCP, based on two observations. (i) The temperature factors of the H4 Q31 residue and the guanine in the H4 K31Q mutant NCP were rather high, as compared to those of the H4 K31 residue and the guanine in the wild-type NCP and the mutant (H3 K79Q or H4 K77Q, see below) NCPs determined at the same resolution (2.7 Å). (ii) The side-chain amines of the H4 R35 residue, which form a salt bridge network with the H4 K31 residue and DNA in the wild-type NCP, face the opposite direction in the H4 K31Q mutant NCP (Figure 5B). The H4 K31Q mutant forms a salt bridge between the H4 R35 and H3 E50 residues (Figure 5B), but it does not induce a large structural change.

Structures of the H4 K77Q and H4 K79Q Mutant NCPs. Peptide mass fingerprinting of bovine histones revealed that the H4 K77 and H4 K79 residues are acetylated.¹⁰ The H4 K79Q substitution leads to a loss of telomeric silencing and rDNA silencing, whereas the H4 K79R substitution has no effect on these phenomena in yeast.⁴⁷ These results suggest that the H4 K79 acetylation may disrupt the heterochromatin structure in telomeric and rDNA loci. On the other hand, the H4 K77Q substitution does not affect telomeric silencing, whereas the H4 K77R substitution increases telomeric silencing.⁴⁷ The H4 K77 and H4 K79 residues are both located on the H4 L2 loop connecting the $\alpha 2$ and $\alpha 3$ helices (Figure 1B). The H4 K77 $\text{N}\varepsilon$ group in the wild-type NCP forms a water-mediated hydrogen bond with the DNA backbone (Figure 6A). This hydrogen bond is missing in the H4 K77Q mutant NCP (Figure 6B), but the impact on the overall structure is minimal.

In the wild-type NCP, the H4 K79 residue forms a hydrogen bond between the main chain amide nitrogen and a DNA

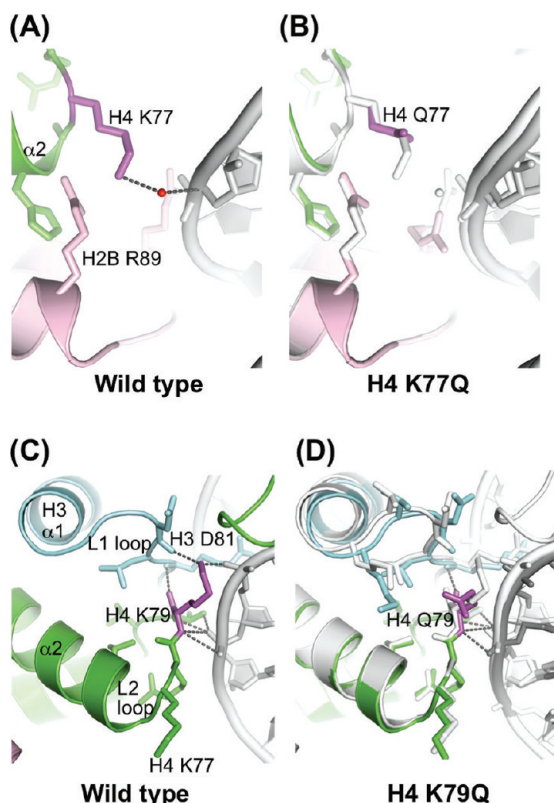


Figure 6. Structures of the H4 K77Q and H4 K79Q mutant NCPs. (A, B) Close-up views of the structures around the H4 K77 residue of the wild-type NCP (A) and the H4 K77Q mutant NCP (B). The H4 K77 (A) and H4 Q77 (B) residues are shown in magenta. (C, D) Close-up views of the structures around the H4 K79 residue of the wild-type NCP (C) and the H4 K79Q mutant NCP (D). The H4 K79 (C) and H4 Q79 (D) residues are shown in magenta. Histones H2B, H3, and H4 are colored pink, cyan, and green, respectively. Hydrogen bonds and salt bridges are denoted by dashed lines. In panels B and D, the wild-type structure is superimposed and shown in white for comparison. Water molecules mediating hydrogen bonds are depicted as red spheres.

backbone phosphate and also forms a salt bridge between the side chain $\text{N}\varepsilon$ and a DNA backbone phosphate (Figure 6C). The H4 K79 $\text{N}\varepsilon$ atom also forms a hydrogen bond with a main chain carbonyl oxygen of the H3 D81 residue in the H3 L1 loop (Figure 6C). In the H4 K79Q mutant NCP, the salt bridge with the DNA and the hydrogen bond with the H3 D81 residue are disrupted, whereas the hydrogen bonds between the main chain amide nitrogen at position 79 and the DNA phosphate are retained (Figure 6D). The acetylated H4 K79 side chain may bend toward the outside of the NCP, as seen in the H4 K79Q mutant side chain because there is no space to accommodate an additional acetyl group on the H4 K79 $\text{N}\varepsilon$ in the original position (Figure 6C,D). Therefore, the acetylation of the H4 K79 residue is predicted to have a similar structural effect as the H4 K79Q mutation.

The loss of the hydrogen bond between H4 K79 and H3 D81 found in the H4 K79Q mutant NCP suggests that the acetylation of the lysine may destabilize the interaction between H4 L2 loop and H3 L1 loop, which compose the DNA binding site. Therefore, the acetylation of the H4 K79 residue may allosterically weaken the histone–DNA interactions, in addition to inhibiting the direct histone–DNA interactions by acetylation.

Structure of the H4 K91Q Mutant NCP. The H4 K91 acetylation was first identified in bovine histones by peptide mass fingerprinting.¹⁰ Subsequently, the acetylation of the H4 K91 residue was also found in yeast histone H4 that was copurified with the nuclear Hat1p–Hat2p–Hif1p complex.⁴⁹ Hat1p/Hat2p, a histone acetyltransferase type B complex, is considered to catalyze the acetylation of newly synthesized histones in the cytoplasm, and Hif1p is an H3/H4-specific histone chaperone that functions in chromatin assembly.⁵⁰ Therefore, it has been proposed that the newly synthesized H4 is acetylated on the K91 residue prior to its deposition onto DNA and that the acetyl group of the H4 K91 residue is deacetylated to allow the H3/H4–H2A/H2B association.⁴⁹

In yeast, the H4 K91Q mutant reportedly exhibited abnormalities in DNA repair and transcriptionally silenced chromatin formation, whereas H4 K91R was apparently normal.^{47,49} In the crystal structure of the human wild-type NCP, the H4 K91 residue forms salt bridges with the H2B D65 residue (Figure 7A). These salt bridges are lost in the H4 K91Q

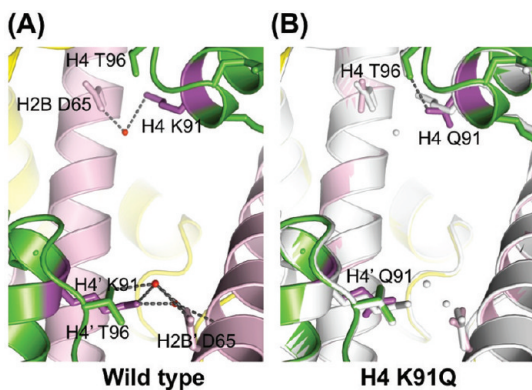


Figure 7. Structure of the H4 K91Q mutant NCP. (A) Close-up view of the structure around the H4 K91 residue of the wild-type NCP. (B) Close-up view of the structure of the H4 K91Q mutant NCP. Histones H2A, H2B, and H4 are colored yellow, pink, and green, respectively. The H4 K91 (A) and H4 Q91 (B) residues are shown in magenta. Hydrogen bonds and salt bridges are denoted by dashed lines. In panel B, the wild-type structure is superimposed and shown in white for comparison. Water molecules mediating hydrogen bonds are depicted as red spheres.

mutant NCP (Figure 7B). However, no changes in the configuration between H4 and H2B are observed in the H4 K91Q mutant NCP, and the overall structural change is very small. The two symmetric H4 K91 residues in the NCP are located at the center of the nucleosomal disk, about 18 Å apart (Figure 1A). These H4 K91 locations may be propitious to change the nucleosome stability, by the loss of the salt bridges at the H4 K91 residue. Therefore, the disruption of the salt bridges at the H4 K91 residue in the H4 K91Q mutant NCP may be responsible for the defective formation of transcriptionally silenced chromatin, as seen in the yeast containing the H4 K91Q mutant.^{47,49}

Yan et al. reported that BBAP E3 ligase monoubiquitinates the H4 K91 residue and confers a protective response to DNA-damaging agents.⁵¹ When BBAP was depleted prior to exposure to the DNA damaging agent doxorubicin, significant decreases of the H4 K20 mono- and dimethylation and an increase of the H4 K91 acetylation were observed.⁵¹ Hence, crosstalk might occur between the acetylation and the ubiquitination at the H4

K91 residue. The H4 K91 residue is located in the interior of the histone octamer, but there is sufficient space for acetyl moieties, if the H4 K91 side chain is placed within the vacant space and avoids the steric clashes with the H2B D65 and H4 T96 residues (Figure 7A). Our study revealed that the H4 K91Q mutant forms an NCP with a similar structure to the wild-type NCP, without salt bridges between the H4 K91 residue and the H2B D65 residue (Figure 7B). The acetylation of the H4 K91 residue in newly synthesized histone H4 may be retained in chromatin, and it may play roles in transcription promotion or the DNA damage response, in a similar manner to the acetylation of the H3 K56 residue.⁵²

Structures of the H3 K79Q and H4 K59Q Mutant NCPs.

The H3 K79 and H4 K59 residues are both exposed on the disk surface of the NCP (Figure 1A). Acetylation at these sites has not been reported, although these lysines are known to be methylated. The H3 K79 methylation is one of the most well-studied modifications in the histone-fold domain and is involved in telomere silencing and meiotic checkpoint control.^{53–55} The crystal structure of the NCP reconstituted with the H3 K79 dimethylated histones revealed that the H3 K79 dimethylation does not affect the conformations of other residues but only alters the side-chain conformation of the H3 K79 residue.⁵⁶ The H3 K79 residue is located at the C-terminal end of the H3 α 1 helix (Figure 8A). In the wild-type NCP, the

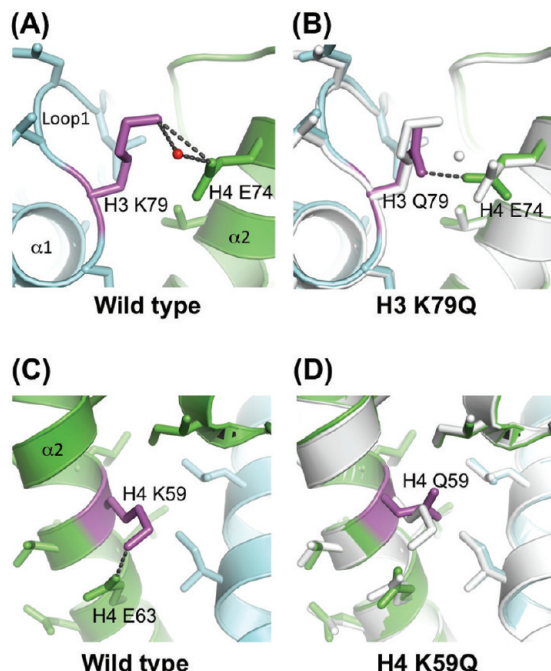


Figure 8. Structures of the H3 K79Q and H4 K59Q mutant NCPs. (A, B) Close-up views of the structures around the H3 K79 residue of the wild-type NCP (A) and the H3 K79Q mutant NCP (B). The H3 K79 (A) and H3 Q79 (B) residues are shown in magenta. (C, D) Close-up views of the structures around the H4 K59 residue of the wild-type NCP (C) and the H4 K59Q mutant NCP (D). The H4 K59 (C) and H4 Q59 (D) residues are shown in magenta. Histones H3 and H4 are colored cyan and green, respectively. Hydrogen bonds and salt bridges are denoted by dashed lines. In panels B and D, the wild-type structure is superimposed and shown in white for comparison. Water molecules mediating hydrogen bonds are depicted as red spheres.

H3 K79 side chain forms salt bridges with the H4 E74 side chain (Figure 8A). On the other hand, in the H3 K79Q mutant

NCP, the salt bridges are absent, but the H3 Q79 side chain newly forms a hydrogen bond with the H4 E74 side chain (Figure 8B). Therefore, the interaction between the H3 K79 and H4 E74 residues is maintained in the H3 K79Q mutant NCP, and the change does not influence the conformations of the proximal residues.

The H4 K59 residue has been identified as a methylation site.¹⁰ The H4 K59A and H4 K59Q mutations lead to a rDNA silencing defect.⁴⁷ This suggests that the positive charge of the H4 K59 residue is necessary for effective rDNA silencing. The H4 K59Q substitution disrupts the H4 K59–E63 interaction observed in the wild-type NCP (Figure 8C,D). However, the loss of the H4 K59–E63 salt bridge only minimally affects the overall structure of the H4 K59Q mutant NCP.

Structure of the H4 K44Q Mutant NCP. No modification of the H4 K44 residue has been reported to date. However, a significant change in the NCP structure with the H4 K44Q mutation was observed in this study. The H4 K44 residue exists on the H4 L1 loop, located near the entry and exit point of the nucleosomal DNA (Figure 1A). The side chain of the adjacent H4 R45 residue protrudes into the minor groove of the DNA, and the H4 V43 residue contributes to the stabilization of the H4 L1 and H3 L2 loops through hydrophobic contacts. Mutations of these amino acid residues (H4 V43I, H4 R45H, H4 R45C) display a Sin phenotype.⁴²

Surprisingly, we found that the electron densities of the two symmetric H2A C-terminal loop regions (H2A I111–K118) are completely absent in the H4 K44Q mutant NCP, although these H2A regions are clearly visible in the wild-type NCP (Figure 9A,B). In the wild-type NCP, the carbonyl oxygen of the H2A L115 residue is located 2.8 Å away from the $\text{N}\varepsilon$ of the H4 K44 side chain, and a hydrogen bond is formed between them (Figure 9C). However, in the structure of the H4 K44Q mutant NCP, the side chain of the substituted glutamine would clash with the H2A L115 residue, if the H2A C-terminal loop retained the same conformation as in the wild-type NCP (Figure 9C,D). This steric hindrance may be the reason why the H2A C-terminal loop is disordered in the H4 K44Q mutant NCP.

The H4 K44 residue reportedly interacts with the Set2 methyltransferase, which di- and trimethylates the H3 K36 residue in *S. cerevisiae*, because the H3 K36 di- and trimethylations are significantly reduced in yeast strains expressing the H4 K44Q mutant.⁵⁷ During transcription elongation in *S. cerevisiae*, the Set2 methyltransferase catalyzes the H3 K36 methylation in chromatin, behind the elongating RNA polymerase II. The methylated H3 K36 residues provide binding sites for the Rpd3S histone deacetylase complex, which *cis*- and *trans*-deacetylates H3 and H4.^{58–61} These deacetylations may restore the chromatin structure after the transit of RNA polymerase II and prevent cryptic intragenic transcription. This process is essential for proper transcription elongation. NSD2, the mammalian homologue of Set2, also exhibits a severe reduction in the H3 K36 methylation in the H4 K44Q mutant nucleosome.⁶² Previous mutational studies suggested that the H4 K44 residue and its proximal H2A L116–L117 residues in *S. cerevisiae* (corresponding to the H2A L115–L116 residues in human) compose the Set2 binding surface on the NCP.^{57,63} In this study, we revealed that the H2A C-terminal loop region (H2A I111–K118) is completely disordered in the H4 K44Q mutant NCP (Figure 9A,B), and the Set2 binding surface is perturbed in the mutant NCP (Figure 9E).

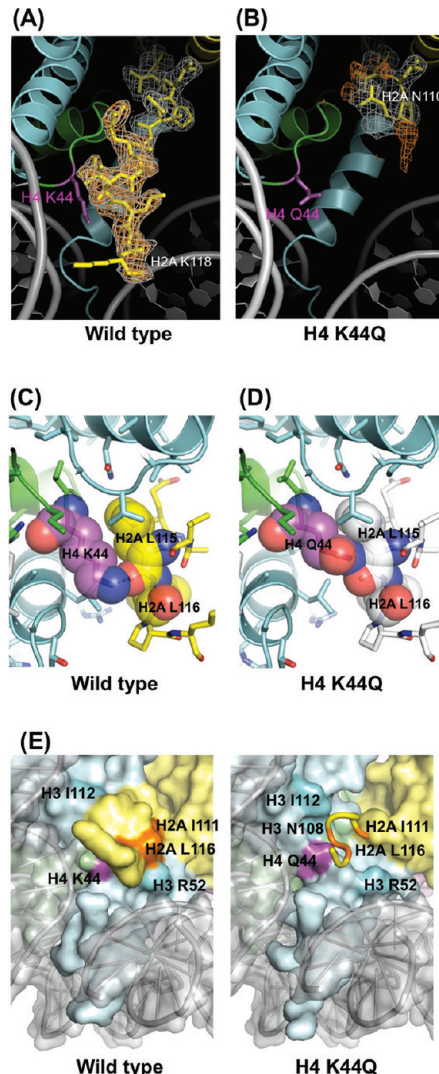


Figure 9. Structure of the H4 K44Q mutant NCP. (A, B) Differences between the wild-type NCP (A) and the H4 K44Q mutant NCP (B) in the electron density maps around the C-terminal region of H2A. $F_0 - F_c$ (contoured at 2.8σ) and $2F_0 - F_c$ (contoured at 1.0σ) omit maps calculated without the H2A N110–K129 residues are shown around the omitted region in orange and white, respectively. The H4 K44 (A) and H4 Q44 (B) residues are shown in magenta. Histones H2A, H3, and H4 are colored yellow, cyan, and green, respectively. (C) Interaction between the H4 K44 residue and the H2A C-terminal loop in the human wild-type NCP. The H4 K44, H2A L115, and H2A L116 residues are shown with van der Waals spheres. Carbon atoms of histones H2A, H3, and H4 are colored yellow, cyan, and green, respectively. (D) Structure of the H4 K44Q mutant NCP in the same orientation as in panel C. Stick and van der Waals models of the H2A N110–K118 residues of the wild-type NCP are superimposed (white carbon atoms). (E) Putative Set2 binding surface of the wild-type NCP (left) and the H4 K44Q mutant NCP (right). The H2A C-terminal loop of the wild-type NCP, which was disordered in the H4 K44Q mutant NCP, is shown as a tube in the right panel for comparison.

Perspective. In the NCP structures determined here, except for the H4 K44Q mutant NCP, local changes at the target sites were observed, but the overall global NCP structures were only moderately altered, as in the previously reported crystal structures of the Sin mutant NCPs,⁴⁵ the chemically H3 K79 dimethylated and H4 K20 trimethylated

NCPs,⁵⁶ the H3 K56Q mutant NCP,²⁰ and the NCPs containing human H3 variants.^{21,29} On the other hand, the histone H2A and H3 variants highly expressed in testis (such as H2A.Bbd, H2AL2, and H3T) and CENP-A reportedly exhibit abnormal stability and nucleosome morphology, in which the DNA ends are quite flexible.^{21,38,64–67} The H3 K56, H3 K64, H3 K115, H3 K122, H4 K31, H4 K77, and H4 K79 residues are known to physically interact with DNA; however, the present structures revealed that the acetyl-mimicking KQ mutations in these residues did not affect the DNA binding path of the nucleosome, unlike the histone variants. Therefore, the histone acetylation may not drastically alter the binding mode of nucleosomal DNA.

The crystal structures of the histone chaperone Asf1 (CIA in human) complexed with histones H3 and/or H4 have been reported.^{68–70} Since the H3 K115, H3 K122, and H4 K91 residues are located near the ASF1–histone interface, acetylations of these residues may reduce the histone binding by ASF1. We found that the H3 K115Q, H3 K122Q, and H4 K91Q substitutions did not significantly affect the overall structure of the NCPs. Therefore, the acetylation of the H3 K115, H3 K122, and H4 K91 residues may function to regulate the interactions with histone chaperones. Further structural studies will clarify this issue.

Interestingly, we found that the H4 K44Q mutation disrupted the H2A C-terminal loop structure by a steric clash and significantly deformed the configuration of the NCP surface, which is thought to interact with the Set2 methyltransferase. The positive charge of the H4 K44 residue is not considered to be essential for interaction with Set2 because the yeast strains expressing H4 K44R, H4 K44A, and H4 K44L exhibited wild-type levels of H3 K36 di- and trimethylation.⁵⁷ Therefore, the perturbation of the H2A C-terminal loop by the H4 K44Q mutation is presumed to inhibit the binding of Set2 to the NCP, which causes the defect in the H3 K36 di- and trimethylation.⁵⁷ A computational prediction from a clustering analysis of the protein sequences identified the H4 K44 residue as a potential acetylation site.⁷¹ If the H4 K44 residue is acetylated, then the increased bulk of the side chain may lead to the perturbation of the H2A C-terminal loop, as seen in the H4 K44Q mutant NCP.

The KQ mutations are frequently employed in genetic, cell biological, and biochemical analyses to understand the functions of lysine acetylation in proteins, especially histones. The present mutant NCP structures have clarified the structural consequences of the KQ mutations in the NCP structures. This is the first comprehensive crystal structural analysis of the mutant NCPs. This study provides fundamental information for future genetic, biochemical, cell biological, and computational analyses, which will elucidate further details toward understanding the regulatory mechanisms of transcription, replication, recombination, and DNA repair in chromatin by the histone PTMs and mutations.

ASSOCIATED CONTENT

Supporting Information

$F_o - F_c$ omit maps for the substituted glutamines in each of the mutant NCPs. This material is available free of charge via the Internet at <http://pubs.acs.org>.

Accession Codes

Coordinates and structure factors have been deposited in the Protein Data Bank (accession codes 3AYW for H3 K56Q,

3AZE for H3 K64Q, 3AZF for H3 K79Q, 3AZG for H3 K115Q, 3AZH for H3 K122Q, 3AZI for H4 K31Q, 3AZJ for H4 K44Q, 3AZK for H4 K59Q, 3AZL for H4 K77Q, 3AZM for H4 K79Q, and 3AZN for H4 K91Q).

AUTHOR INFORMATION

Corresponding Author

*Tel: +81-3-5369-7315. Fax: +81-3-5367-2820. E-mail: kurumizaka@waseda.jp.

Author Contributions

[§]The first two authors contributed equally to this work.

Funding

This work was supported in part by Grants-in-Aid from the Japanese Society for the Promotion of Science (JSPS) and the Ministry of Education, Culture, Sports, Science and Technology (MEXT), Japan. H.K. was also supported by the Waseda Research Institute for Science and Engineering.

ACKNOWLEDGMENTS

We express our gratitude to the beamline staff at BL41XU of SPring-8 for their help in data collection.

ABBREVIATIONS

NCP, nucleosome core particle; PTM, post-translational modification; rmsd, root-mean-square deviation; PDB, Protein Data Bank; FRET, fluorescence resonance energy transfer.

REFERENCES

- (1) Luger, K., Mäder, A. W., Richmond, R. K., Sargent, D. F., and Richmond, T. J. (1997) Crystal structure of the nucleosome core particle at 2.8 Å resolution. *Nature* 389, 251–260.
- (2) Arents, G., Burlingame, R. W., Wang, B. C., Love, W. E., and Moudrianakis, E. N. (1991) The nucleosomal core histone octamer at 3.1 Å resolution: a tripartite protein assembly and a left-handed superhelix. *Proc. Natl. Acad. Sci. U. S. A.* 88, 10148–10152.
- (3) Arents, G., and Moudrianakis, E. N. (1995) The histone fold: a ubiquitous architectural motif utilized in DNA compaction and protein dimerization. *Proc. Natl. Acad. Sci. U. S. A.* 92, 11170–11174.
- (4) Strahl, B. D., and Allis, C. D. (2000) The language of covalent histone modifications. *Nature* 403, 41–45.
- (5) Jenuwein, T., and Allis, C. D. (2001) Translating the histone code. *Science* 293, 1074–1080.
- (6) Loyola, A., Bonaldi, T., Roche, D., Imhof, A., and Almouzni, G. (2006) PTMs on H3 variants before chromatin assembly potentiate their final epigenetic state. *Mol. Cell* 24, 309–316.
- (7) Loyola, A., and Almouzni, G. (2007) Marking histone H3 variants: How, when and why? *Trends Biochem. Sci.* 32, 425–433.
- (8) Zhang, K., Tang, H., Huang, L., Blankenship, J. W., Jones, P. R., Xiang, F., Yau, P. M., and Burlingame, A. L. (2002) Identification of acetylation and methylation sites of histone H3 from chicken erythrocytes by high-accuracy matrix-assisted laser desorption ionization-time-of-flight, matrix-assisted laser desorption ionization-postsource decay, and nanoelectrospray ionization tandem mass spectrometry. *Anal. Biochem.* 306, 259–269.
- (9) Cocklin, R. R., and Wang, M. (2003) Identification of methylation and acetylation sites on mouse histone H3 using matrix-assisted laser desorption/ionization time-of-flight and nanoelectrospray ionization tandem mass spectrometry. *J. Protein Chem.* 22, 327–334.
- (10) Zhang, L., Eugeni, E. E., Parthun, M. R., and Freitas, M. A. (2003) Identification of novel histone post-translational modifications by peptide mass fingerprinting. *Chromosoma* 112, 77–86.

- (11) Freitas, M. A., Sklenar, A. R., and Parthun, M. R. (2004) Application of mass spectrometry to the identification and quantification of histone post-translational modifications. *J. Cell. Biochem.* 92, 691–700.
- (12) Cosgrove, M. S., Boeke, J. D., and Wolberger, C. (2004) Regulated nucleosome mobility and the histone code. *Nat. Struct. Mol. Biol.* 11, 1037–1043.
- (13) Mersfelder, E. L., and Parthun, M. R. (2006) The tale beyond the tail: histone core domain modifications and the regulation of chromatin structure. *Nucleic Acids Res.* 34, 2653–2662.
- (14) Neumann, H., Peak-Chew, S. Y., and Chin, J. W. (2008) Genetically encoding N(epsilon)-acetyllysine in recombinant proteins. *Nat. Chem. Biol.* 4, 232–234.
- (15) Neumann, H., Hancock, S. M., Buning, R., Routh, A., Chapman, L., Somers, J., Owen-Hughes, T., van Noort, J., Rhodes, D., and Chin, J. W. (2009) A method for genetically installing site-specific acetylation in recombinant histones defines the effects of H3 K56 acetylation. *Mol. Cell* 36, 153–163.
- (16) Shimko, J. C., North, J. A., Bruns, A. N., Poirier, M. G., and Ottesen, J. J. (2011) Preparation of fully synthetic histone H3 reveals that acetyl-lysine 56 facilitates protein binding within nucleosomes. *J. Mol. Biol.* 408, 187–204.
- (17) Megee, P. C., Morgan, B. A., Mittman, B. A., and Smith, M. M. (1990) Genetic analysis of histone H4: essential role of lysines subject to reversible acetylation. *Science* 247, 841–845.
- (18) Zhang, W., Bone, J. R., Edmondson, D. G., Turner, B. M., and Roth, S. Y. (1998) Essential and redundant functions of histone acetylation revealed by mutation of target lysines and loss of the Gcn5p acetyltransferase. *EMBO J.* 17, 3155–3167.
- (19) Wang, X., and Hayes, J. J. (2008) Acetylation mimics within individual core histone tail domains indicate distinct roles in regulating the stability of higher-order chromatin structure. *Mol. Cell. Biol.* 28, 227–236.
- (20) Watanabe, S., Resch, M., Lilyestrom, W., Clark, N., Hansen, J. C., Peterson, C., and Luger, K. (2010) Structural characterization of H3K56Q nucleosomes and nucleosomal arrays. *Biochim. Biophys. Acta* 1799, 480–486.
- (21) Tachiwana, H., Kagawa, W., Osakabe, A., Kawaguchi, K., Shiga, T., Hayashi-Takanaka, Y., Kimura, H., and Kurumizaka, H. (2010) Structural basis of instability of the nucleosome containing a testis-specific histone variant, human H3T. *Proc. Natl. Acad. Sci. U. S. A.* 107, 10454–10459.
- (22) Otwinowski, Z., and Minor, W. (1997) Processing of X-ray diffraction data collected in oscillation mode. *Methods Enzymol.* 276, 307–326.
- (23) Collaborative Computational Project Number 4. (1994) The CCP4 suite: programs for protein crystallography. *Acta Crystallogr., Sect. D: Biol. Crystallogr.* 50, 760–763.
- (24) Vagin, A., and Teplyakov, A. (1997) MOLREP: an Automated Program for Molecular Replacement. *J. Appl. Crystallogr.* 30, 1022–1025.
- (25) Emsley, P., and Cowtan, K. (2004) Coot: model-building tools for molecular graphics. *Acta Crystallogr., Sect. D: Biol. Crystallogr.* 60, 2126–2132.
- (26) Brünger, A. T., Adams, P. D., Clore, G. M., DeLano, W. L., Gros, P., Grosse-Kunstleve, R. W., Jiang, J. S., Kuszewski, J., Nilges, M., Pannu, N. S., Read, R. J., Rice, L. M., Simonson, T., and Warren, G. L. (1998) Crystallography and NMR system: A new software suite for macromolecular structure determination. *Acta Crystallogr., Sect. D: Biol. Crystallogr.* 54, 905–921.
- (27) DeLano, W. L. (2008) The PyMOL Molecular Graphics System, DeLano Scientific LLC, Palo Alto, CA.
- (28) Tanaka, Y., Tawaramoto-Sasanuma, M., Kawaguchi, S., Ohta, T., Yoda, K., Kurumizaka, H., and Yokoyama, S. (2004) Expression and purification of recombinant human histones. *Methods* 33, 3–11.
- (29) Tachiwana, H., Osakabe, A., Shiga, T., Miya, Y., Kimura, H., Kagawa, W., and Kurumizaka, H. (2011) Crystal structures of human nucleosomes containing major histone H3 variants. *Acta Crystallogr., Sect. D: Biol. Crystallogr.* 67, 578–583.
- (30) Luger, K., Rechsteiner, T. J., and Richmond, T. J. (1999) Preparation of nucleosome core particle from recombinant histones. *Methods Enzymol.* 304, 3–19.
- (31) Davey, C. A., Sargent, D. F., Luger, K., Maeder, A. W., and Richmond, T. J. (2002) Solvent mediated interactions in the structure of the nucleosome core particle at 1.9 Å resolution. *J. Mol. Biol.* 319, 1097–1113.
- (32) Tsunaka, Y., Kajimura, N., Tate, S., and Morikawa, K. (2005) Alteration of the nucleosomal DNA path in the crystal structure of a human nucleosome core particle. *Nucleic Acids Res.* 33, 3424–3434.
- (33) Masumoto, H., Hawke, D., Kobayashi, R., and Verreault, A. (2005) A role for cell-cycle-regulated histone H3 lysine 56 acetylation in the DNA damage response. *Nature* 436, 294–298.
- (34) Xu, F., Zhang, K., and Grunstein, M. (2005) Acetylation in histone H3 globular domain regulates gene expression in yeast. *Cell* 121, 375–385.
- (35) Rufiange, A., Jacques, P. E., Bhat, W., Robert, F., and Nourani, A. (2007) Genome-wide replication-independent histone H3 exchange occurs predominantly at promoters and implicates H3 K56 acetylation and Asf1. *Mol. Cell* 27, 393–405.
- (36) Chen, C. C., Carson, J. J., Feser, J., Tamburini, B., Zabaronick, S., Linger, J., and Tyler, J. K. (2008) Acetylated lysine 56 on histone H3 drives chromatin assembly after repair and signals for the completion of repair. *Cell* 134, 231–243.
- (37) Li, Q., Zhou, H., Wurtele, H., Davies, B., Horazdovsky, B., Verreault, A., and Zhang, Z. (2008) Acetylation of histone H3 lysine 56 regulates replication-coupled nucleosome assembly. *Cell* 134, 244–255.
- (38) Tachiwana, H., Kagawa, W., Shiga, T., Osakabe, A., Miya, Y., Saito, K., Hayashi-Takanaka, Y., Oda, T., Sato, M., Park, S. Y., Kimura, H., and Kurumizaka, H. (2011) Crystal structure of the human centromeric nucleosome containing CENP-A. *Nature* 476, 232–235.
- (39) Garcia, B. A., Hake, S. B., Diaz, R. L., Kauer, M., Morris, S. A., Recht, J., Shabanowitz, J., Mishra, N., Strahl, B. D., Allis, C. D., and Hunt, D. F. (2007) Organismal differences in post-translational modifications in histones H3 and H4. *J. Biol. Chem.* 282, 7641–7655.
- (40) Singh, P., Cho, J., Tsai, S. Y., Rivas, G. E., Larson, G. P., and Szabó, P. E. (2010) Coordinated allele-specific histone acetylation at the differentially methylated regions of imprinted genes. *Nucleic Acids Res.* 38, 7974–7990.
- (41) Daujat, S., Weiss, T., Mohn, F., Lange, U. C., Ziegler-Birling, C., Zeissler, U., Lappe, M., Schübeler, D., Torres-Padilla, M. E., and Schneider, R. (2009) H3K64 trimethylation marks heterochromatin and is dynamically remodeled during developmental reprogramming. *Nat. Struct. Mol. Biol.* 16, 777–781.
- (42) Kruger, W., Peterson, C. L., Sil, A., Coburn, C., Arents, G., Moudrianakis, E. N., and Herskowitz, I. (1995) Amino acid substitutions in the structured domains of histones H3 and H4 partially relieve the requirement of the yeast SWI/SNF complex for transcription. *Genes Dev.* 9, 2770–2779.
- (43) Kurumizaka, H., and Wolffe, A. P. (1997) Sin mutations of histone H3: influence on nucleosome core structure and function. *Mol. Cell. Biol.* 17, 6953–6969.
- (44) Wechsler, M. A., Kladde, M. P., Alfieri, J. A., and Peterson, C. L. (1997) Effects of Sin versions of histone H4 on yeast chromatin structure and function. *EMBO J.* 16, 2086–2095.
- (45) Muthurajan, U. M., Bao, Y., Forsberg, L. J., Edayathumangalam, R. S., Dyer, P. N., White, C. L., and Luger, K. (2004) Crystal structures of histone Sin mutant nucleosomes reveal altered protein-DNA interactions. *EMBO J.* 23, 260–271.
- (46) Manohar, M., Mooney, A. M., North, J. A., Nakkula, R. J., Picking, J. W., Edon, A., Fishel, R., Poirier, M. G., and Ottesen, J. J.

- (2009) Acetylation of histone H3 at the nucleosome dyad alters DNA-histone binding. *J. Biol. Chem.* 284, 23312–23321.
- (47) Hyland, E. M., Cosgrove, M. S., Molina, H., Wang, D., Pandey, A., Cottie, R. J., and Boeke, J. D. (2005) Insights into the role of histone H3 and histone H4 core modifiable residues in *Saccharomyces cerevisiae*. *Mol. Cell. Biol.* 25, 10060–10070.
- (48) Garcia, B. A., Busby, S. A., Shabanowitz, J., Hunt, D. F., and Mishra, N. (2005) Resetting the epigenetic histone code in the MRL-lpr/lpr mouse model of lupus by histone deacetylase inhibition. *J. Proteome Res.* 4, 2032–2042.
- (49) Ye, J., Ai, X., Eugeni, E. E., Zhang, L., Carpenter, L. R., Jelinek, M. A., Freitas, M. A., and Parthun, M. R. (2005) Histone H4 lysine 91 acetylation a core domain modification associated with chromatin assembly. *Mol. Cell* 18, 123–130.
- (50) Ai, X., and Parthun, M. R. (2004) The nuclear Hat1p/Hat2p complex: a molecular link between type B histone acetyltransferases and chromatin assembly. *Mol. Cell* 14, 195–205.
- (51) Yan, Q., Dutt, S., Xu, R., Graves, K., Juszczynski, P., Manis, J. P., and Shipp, M. A. (2009) BBAP monoubiquitylates histone H4 at lysine 91 and selectively modulates the DNA damage response. *Mol. Cell* 36, 110–120.
- (52) Schwartz, B. E., and Ahmad, K. (2006) Chromatin Assembly with H3 Histones: Full Throttle Down Multiple Pathways. *Curr. Top. Dev. Biol.* 74, 31–55.
- (53) Feng, Q., Wang, H., Ng, H. H., Erdjument-Bromage, H., Tempst, P., Struhl, K., and Zhang, Y. (2002) Methylation of H3-lysine 79 is mediated by a new family of HMTases without a SET domain. *Curr. Biol.* 12, 1052–1058.
- (54) Krogan, N. J., Dover, J., Wood, A., Schneider, J., Heidt, J., Boateng, M. A., Dean, K., Ryan, O. W., Golshani, A., Johnston, M., Greenblatt, J. F., and Shilatifard, A. (2003) The Paf1 complex is required for histone H3 methylation by COMPASS and Dot1p: linking transcriptional elongation to histone methylation. *Mol. Cell* 11, 721–729.
- (55) Huyen, Y., Zgheib, O., Ditullio, R. A., Gorgoulis, V. G., Zacharatos, P., Petty, T. J., Sheston, E. A., Mellert, H. S., Stavridi, E. S., and Halazonetis, T. D. (2004) Methylated lysine 79 of histone H3 targets 53BP1 to DNA double-strand breaks. *Nature* 432, 406–411.
- (56) Lu, X., Simon, M. D., Chodaparambil, J. V., Hansen, J. C., Shokat, K. M., and Luger, K. (2008) The effect of H3K79 dimethylation and H4K20 trimethylation on nucleosome and chromatin structure. *Nat. Struct. Mol. Biol.* 15, 1122–1124.
- (57) Du, H. N., Fingerman, I. M., and Briggs, S. D. (2008) Histone H3 K36 methylation is mediated by a trans-histone methylation pathway involving an interaction between Set2 and histone H4. *Genes Dev.* 22, 2786–2798.
- (58) Carrozza, M. J., Li, B., Florens, L., Saganuma, T., Swanson, S. K., Lee, K. K., Shia, W. J., Anderson, S., Yates, J., Washburn, M. P., and Workman, J. L. (2005) Histone H3 methylation by Set2 directs deacetylation of coding regions by Rpd3S to suppress spurious intragenic transcription. *Cell* 123, 581–592.
- (59) Joshi, A. A., and Struhl, K. (2005) Eaf3 chromodomain interaction with methylated H3-K36 links histone deacetylation to Pol II elongation. *Mol. Cell* 20, 971–978.
- (60) Keogh, M. C., Kurdistani, S. K., Morris, S. A., Ahn, S. H., Podolny, V., Collins, S. R., Schuldiner, M., Chin, K., Punna, T., Thompson, N. J., Boone, C., Emili, A., Weissman, J. S., Hughes, T. R., Strahl, B. D., Grunstein, M., Greenblatt, J. F., Buratowski, S., and Krogan, N. J. (2005) Cotranscriptional set2 methylation of histone H3 lysine 36 recruits a repressive Rpd3 complex. *Cell* 123, 593–605.
- (61) Li, B., Gogol, M., Carey, M., Lee, D., Seidel, C., and Workman, J. L. (2007) Combined action of PHD and chromo domains directs the Rpd3S HDAC to transcribed chromatin. *Science* 316, 1050–1054.
- (62) Li, Y., Trojer, P., Xu, C. F., Cheung, P., Kuo, A., Drury, W. J. 3rd, Qiao, Q., Neubert, T. A., Xu, R. M., Gozani, O., and Reinberg, D. (2009) The target of the NSD family of histone lysine methyltransferases depends on the nature of the substrate. *J. Biol. Chem.* 284, 34283–34295.
- (63) Du, H. N., and Briggs, S. D. (2010) A nucleosome surface formed by histone H4, H2A, and H3 residues is needed for proper histone H3 Lys36 methylation, histone acetylation, and repression of cryptic transcription. *J. Biol. Chem.* 285, 11704–11713.
- (64) Gautier, T., Abbott, D. W., Molla, A., Verdel, A., Ausio, J., and Dimitrov, S. (2004) Histone variant H2ABbd confers lower stability to the nucleosome. *EMBO Rep.* 5, 715–720.
- (65) Bao, Y., Konesky, K., Park, Y. J., Rosu, S., Dyer, P. N., Rangasamy, D., Tremethick, D. J., Laybourn, P., and Luger, K. (2004) Nucleosomes containing the histone variant H2A.Bbd organize only 118 base pairs of DNA. *EMBO J.* 23, 3314–3324.
- (66) Doyen, C. -M., Montel, F., Gautier, T., Menoni, H., Claudet, C., Delacour-Larose, M., Angelov, D., Hamiche, A., Bednar, J., Faivre-Moskalenko, C., Bouvet, P., and Dimitrov, S. (2006) Dissection of the unusual structural and functional properties of the variant H2A.Bbd nucleosome. *EMBO J.* 25, 4234–4244.
- (67) Syed, S. H., Boulard, M., Shukla, M. S., Gautier, T., Travers, A., Bednar, J., Faivre-Moskalenko, C., Dimitrov, S., and Angelov, D. (2009) The incorporation of the novel histone variant H2AL2 confers unusual structural and functional properties of the nucleosome. *Nucleic Acids Res.* 37, 4684–4695.
- (68) English, C.M., Adkins, M. W., Carson, J. J., Churchill, M. E. A., and Tyler, J. K. (2006) Structural basis for the histone chaperone activity of Asf1. *Cell* 127, 495–508.
- (69) Antczak, A. J., Tsubota, T., Kaufman, P. D. Berger, J. M. (2006) Structure of the yeast histone H3-ASF1 interaction: implications for chaperone mechanism, species-specific interactions, and epigenetics. *BMC Struct. Biol.* 6:26.
- (70) Natsume, R., Eitoku, M., Akai, Y., Sano, N., Horikoshi, M., and Senda, T. (2007) Structure and function of the histone chaperone CIA/ASF1 complexed with histones H3 and H4. *Nature* 446, 338–341.
- (71) Basu, A., Rose, K. L., Zhang, J., Beavis, R. C., Ueberheide, B., Garcia, B. A., Chait, B., Zhao, Y., Hunt, D. F., Segal, E., Allis, C. D., and Hake, S. B. (2009) Proteome-wide prediction of acetylation substrates. *Proc. Natl. Acad. Sci. U. S. A.* 106, 13785–13790.